ELSEVIER

Biochimica et Biophysica Acta 1420 (1999) 14–22

BIOCHIMICA ET BIOPHYSICA ACTA
BBA

www.elsevier.com/locate/bba

C-terminally shortened alamethicin on templates: influence of the linkers on conductances

Hervé Duclohier [a,*], Karol Kociolek [b], Marcin Stasiak [b], Miroslaw T. Leplawy [b], Garland R. Marshall [c]

[a] *UMR 6522 CNRS-Université de Rouen, Institut Fédératif de Recherches Multidisciplinaires sur les Peptides (IFRMP 23), 76821 Mont-Saint-Aignan, Cedex, France*

[b] *Institute of Organic Chemistry, Technical University of Lodz, Zeromski Str. 116, 90-924 Lodz, Poland*

[c] *Department of Molecular Biology and Pharmacology, Washington University School of Medicine, St. Louis, MO 63110, USA*

Received 17 November 1998; received in revised form 8 March 1999; accepted 18 March 1999

Abstract

In order to test the influence of chemical modifications designed to allow covalent coupling of channel-forming peptide motifs into variable sized oligomers, a series of alamethicin derivatives was prepared. The building block encompassing the N-terminal 1–17 residues of alamethicin behaved normally in the conductance assay on planar lipid bilayers, albeit at higher concentration and with a slightly reduced voltage-dependence. A linker Ac-K-$OCH_2C_6H_4CH_3p$ attached via the epsilon amino group of lysine to the C-terminus of alamethicin(1–17) increased membrane affinity. The latter was further enhanced in a dimer and a tetramer in which alamethicin(1–17) chains were tethered to di- or tetra-lysine linkers, respectively, but macroscopic current–voltage curves displayed much reduced voltage-dependencies and reversed hysteresis. An usual behaviour with high voltage-dependence was restored with the modified dimer of alamethicin(1–17) in which alanine separated the two consecutive lysine residues in the linker. Of special interest was the development of a 'negative resistance' branch in macroscopic current–voltage curves for low concentrations of this dimer with the more flexible linker. Single channel events displayed only one single open state with fast kinetics and whose conductance matches that of the alamethicin heptamer or octamer.

Keywords: Alamethicin oligomer; Peptaibol; Voltage-gated channel; Conductance; Planar lipid bilayer

1. Introduction

Alamethicin is a peptaibol antibiotic of 20 residues, rich in α-aminoisobutyric acid (Aib, U or α-methylalanine, MeA), whose ability to form pores in planar lipid bilayers has been studied for a number of years [1–3] (and for reviews, see [4–6]). Pore formation by alamethicin is characterised by both a high voltage-dependence of its macroscopic conductance reflecting the steep recruitment of many channels [7,8] and multiple open states at the single-channel level, whose conductances obey a geometrical progression [9,10]. The dynamic 'barrel-stave' model [11] in which the release of amphipathic alamethicin

Abbreviations: Boc, *t*-butoxycarbonyl; Bzl, benzyl; DMF, dimethylformamide; Fmoc, 9-fluorenylmethoxycarbonyl; HOBt, hydroxybenzotriazol; TBTU, *N*[(1*H*-benzotriazol-1-yl)(dimethylamino)methylene]-*N*-methyl-methanaminum tetrafluoroborate *N*-oxide; U, α-aminoisobutyric acid or α-methylalanine

* Corresponding author. Fax: +33-2-3514-6704;
E-mail: herve.duclohier@univ-rouen.fr

0005-2736/99/$ – see front matter
PII: S0005-2736(99)00047-4

monomers account for the multi-state behaviour now serves as a paradigm for many other pore formers (for review see [12]), although the open channel structure itself still remains a matter of debate [6,13].

The preparation of covalently bound oligomers of alamethicin has been an active field of research in recent years [14–16]. One of the main goals is to assign a particular conductance state to a given geometry of the conducting bundle in accord with the high voltage-dependence of pore-formation. The template approach in assembling functional motifs in well-defined spatial arrangements [17] has been applied with some success in oligomers mimicking the pore region of physiological channels such as the dihydropyridine-sensitive calcium channel [18] and the acetylcholine receptor [19]. In the case of alamethicin, templates most often showed a significantly reduced voltage-dependence [16]. In general, and apart from a recent study assaying different rigid aromatic templates for their capacity to enhance the helicity of an amphipathic peptide [20], little attention has been paid to the influence of the linkers on the resulting properties of covalent oligomers as compared to that of self-assembled monomers.

We herein report the chemical synthesis and comparative conductance assays of a series of alamethicin derivatives tethered to different linkers. In some cases, specifically when more flexibility was provided, a high voltage-sensitivity was preserved and decoupled from the multi-state behaviour. In addition, other interesting features such as 'negative resistance', a signature of regenerative or excitable systems were much easier to obtain than with native alamethicin.

2. Materials and methods

2.1. Peptide synthesis

Formulas and analytical data of alamethicin derivatives and oligomers are shown in Fig. 1 and Table 1, respectively.

2.1.1. Alamethicin(1–17) (**1**)

We used the Boc/OBzl protection strategy, TBTU or TBTU/HOBt coupling reagents and solution synthesis protocol throughout the preparation of all intermediate peptides (1–3+4–5)+(6–8+9–11) and (12–14+15–17). The acyl donor segments had racemisation resistant or achiral residues (U, P, G) on their C-termini. In the final condensation step, the acyl donor and acceptor segments (1–11)-OH and (12–17)-OBzl having C-terminal G and N-terminal L, respectively, were coupled (12 h) on an unprecedented gram scale by means of TBTU in DMF affording nearly pure alamethicin(1–17)-OBzl in a yield of 90%. After debenzylation (H_2/Pd/CH_3OH) and recrystallisation (AcOEt/MeOH/hexane), the obtained alamethicin(1–17) was chromatographically identical with a highly pure standard sample of alamethicin prepared via enzymatic segment condensation [21]. The chemical methodology to overcome synthetic difficulties in the preparation of alamethicin segments is discussed in previous papers [21–25] on the total solution synthesis of this peptaibol antibiotic.

2.1.2. Alamethicin(1–17)-AUA (**2**)

Coupling of Boc-(12–17)-OH segment and A-U-A-OBzl tripeptide in equimolar amounts (TBTU, DMF, 48 h) afforded Boc-(12–20)-OBzl nonapeptide. After deprotection, this was condensed with Ac-(1–11)-OH in analogy to alamethicin(1–17). The yield was 91%

2.1.3. Monomer **3**, dimer **4** and tetramer **6**

All couplings were performed (20 h) using TBTU/HOBt activation in DMF as a solvent. Boc-K(Fmoc)-OH was transformed into Boc-K-$OCH_2C_6H_4CH_3p$ which was further used for derivatisation of (1–17)alamethicin to furnish the key intermediate Boc-K(ε-1–17alamethicin)-$OCH_2C_6H_4CH_3p$. Replacement of Boc protection by the acetyl group afforded monomer **3**. After separately performed C-deprotection and N-deprotection, the two building blocks Boc-K(ε-1-17alamethicin)-OH and H-K(ε-1–17alamethicin)-$OCH_2C_6H_4CH_3p$ for construction of the dimer were obtained. They were coupled to give covalently bound dimer **4** (in Boc-derivative form) with simultaneous formation of the dilysine template. After hydrogenolytic cleavage of the benzyl ester group, the dimer with free carboxylic group and the monomeric derivative H-K(ε-1-17alamethicin)-$OCH_2C_6H_4C_H3p$ were used for stepwise assembly in DMF solution of the covalently bound trimer

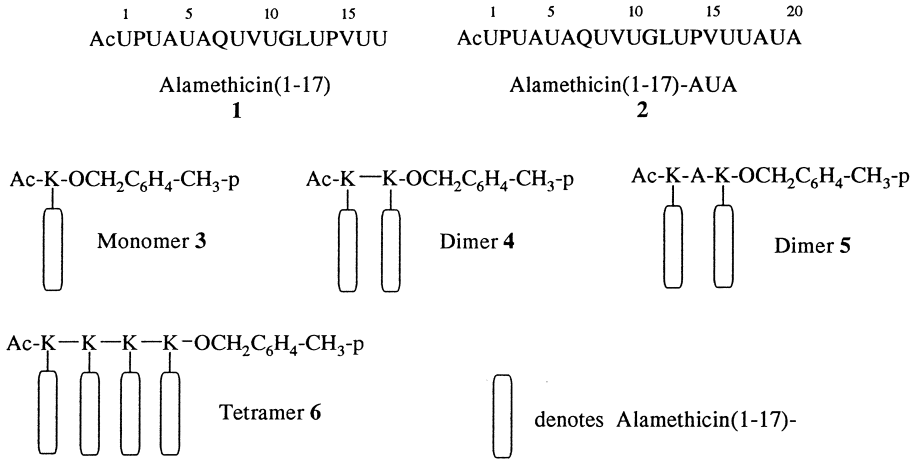

Fig. 1. Alamethicin derivatives and oligomers of (1–17)alamethicin on templates. Products are referred in the text by the bold numbers shown in this figure and the table below. The building block **1**, encompassing N-terminal 1–17 residues of alamethicin is attached to the ε-amino group of lysine yielding monomer **3**. Two or four contiguous lysines allow the construction of dimer **4** or tetramer **6**. In another dimer (**5**), there is an intervening alanine between the two lysines.

Table 1
Analytical data of alamethicin derivatives and oligomers

Compounds	MW (nominal)/MW (chemical)	MS (*m/z*)	Purity by HPLC[a] (%)	HPLC data[a]
Alamethicin(1–17) (**1**) $C_{73}H_{124}N_{18}O_{20}$	1572 1573.90	1571 $[M-H]^-$ LSIMS(−)	100	Column: Vydac RP-C18 (0.46×25 cm) R_T = 8.47 min, 60% B (isocratic) R_T = 13.09 min, 50–80% B 25 min
Alamethicin(1–17)-AUA (**2**) $C_{83}H_{141}N_{21}O_{23}$	1799 1801.16	1823 $[MNa]^+$ 1839 $[MK]^+$ LSIMS(+)	100	Column: Vydac RP-C18 (0.46×25 cm) R_T = 12.53 min, 65% (isocratic) R_T = 9.01 min, 70% (isocratic)
Monomer **3** $C_{89}H_{146}N_{20}O_{22}$	1846 1848.26	1848 $[MH]^+$ 1871 $[MNa]^+$ 1887 $[MK]^+$ LSIMS(+)	>95	Column: Vydac RP-C18 (0.46×25 cm) R_T = 12.34 min, 75–90% B 25 min Column: Vydac RP-C4 (0.46×25 cm) R_T = 5.92 min, 75–90% B 25 min
Dimer **4** $C_{168}H_{280}N_{40}O_{42}$	3528 3532.31	3530.3 $[MH]^+$ 3553.3 $[MNa]^+$ 3569.1 $[MK]^+$ LSIMS(+)	100	Column: Vydac RP-C4 (0.46×25 cm) R_T = 12.67 min, 75–90% B 25 min
Dimer **5** $C_{171}H_{284}N_{41}O_{43}$	3598 3602.38	3601.7 $[MH]^+$ 3625.8 $[MNa]^+$ LSIMS(+)	100	Column: Vydac RP-C4 (0.46×25 cm) R_T = 10.33 min, 75–90% B 25 min R_T = 7.66 min, 80–95% B 25 min
Tetramer **6** $C_{327}H_{548}N_{80}O_{82}$	6904 6912.43	6937 $[MNa]^+$ MALDI	>70	Column: Vydac RP-C4 (0.46×25 cm) R_T = 17.16 min, 85–100% B 25 min R_T = 10.41 min, 100% B (isocratic)

[a]Chromatograph: LDC. Detection: UV 220 nm. Solvents: A, H_2O+0.05% TFA; B, 90% CH_3CN/10% H_2O+0.038% TFA. Flow rate: 1 ml/min.

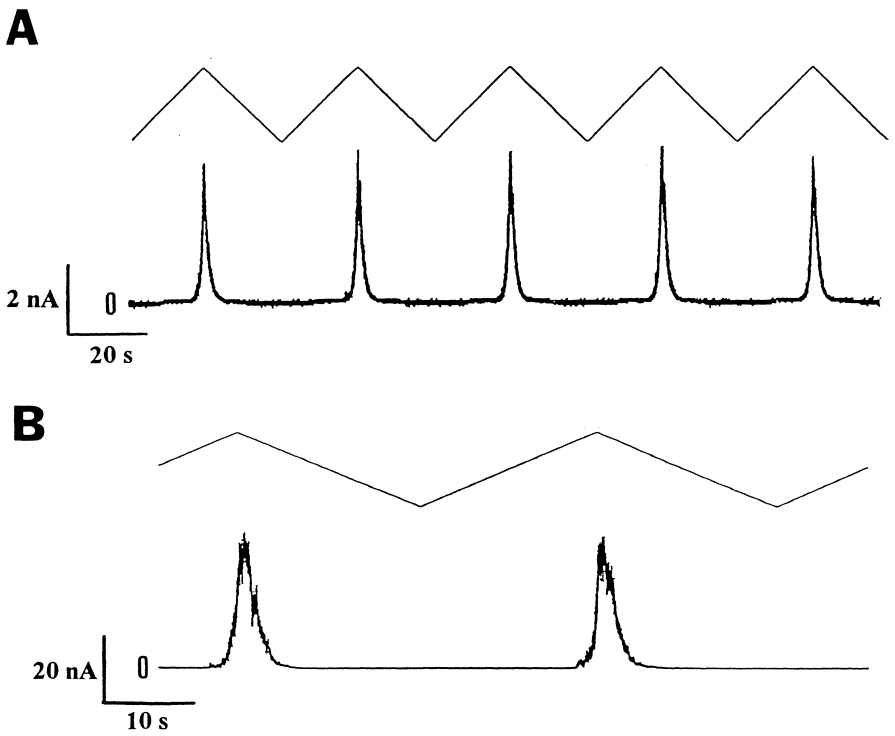

Fig. 2. Successive macroscopic current responses to slow voltage ramps of 140 mV (shown by the upper traces) induced by derivatives **1** and **2** (A and B, respectively). Peptide bath (*cis*-side) concentrations were 3×10^{-7} and 10^{-7} M, respectively. The electrolyte was 0.5 M KCl both sides of a POPC/DOPE (7/3) bilayer. Note the different ranges of current amplitudes.

and tetramer **6**. Final products were purified by size exclusion chromatography, Sephadex LH-20, column (110×2.5 cm), methanol, 6–8 drops/min.

In this synthesis, only the first of four couplings was performed using acetylated peptide with C-terminal sterically hindered and slowly reacting α-aminoisobutyric acid. A further advantage of this strategy is the controlled assembly of the dimer, trimer, tetramer in one synthetic run. Any deletion sequence differs from the desired product by at least 18 amino acid residues which makes purification by size exclusion chromatography efficient.

*2.1.4. Dimer on K-A-K template (**5**)*

This dimer was prepared in an analogous manner as the dimer **4** except that Boc-A-OH was attached to the ε-amino group of lysine at the H-K(ε-1-17alamethicin)-$OCH_2C_6H_4CH_3p$ stage.

2.2. Conductance assays in planar lipid bilayers

Conductance assays, both at the macroscopic (or 'many-channels') conductance and at single-channel levels, were performed after equilibration of the derivatives with virtually solvent-free planar lipid bilayers ('folded' or Montal–Mueller type [26]). A mixture of neutral lipids from Avanti Polar Lipids (Alabaster, AL, USA), 1-palmitoyl-2-oleoyl-*sn*-glycero-3-phosphocholine (POPC) and 1,2-dioleoyl-*sn*-glycero-3-phosphoethanolamine (DOPE) with the ratio 7/3 (w/w) was used as a rule to form the monolayers. The latter were formed by spreading the lipids dissolved in hexane (10 mg/ml) on top of the electrolyte (either 0.5 or 1 M KCl) both sides of the chamber. After solvent evaporation, bilayer formation was achieved by lowering, then raising back, the electrolyte level in front of a 200-μm hole in the PTFE septum. After control of the bilayer stability and electrical silence under applied voltage, derivatives were added to the *cis*-side of the chamber from a methanolic stock solution (final MeOH concentration below 1%). Bilayers were then either submitted to slow voltage ramps for recording macroscopic current–voltage curves, or to steady-state voltages for

single-channel traces. Currents were amplified via a current-to-voltage converter (Keithley model 427; Cleveland, OH) and traces were delivered either as a function of time or as a function of voltage (current–voltage or *I–V* curves, *X–Y* plotter from Linseis, model 1600).

3. Results

Macroscopic current responses to identical voltage ramps of alamethicin(1–17) (**1**) and its extended form alamethicin(1–17)-AUA (**2**) are compared in Fig. 2A and B. In both cases, the usual behaviour typical of

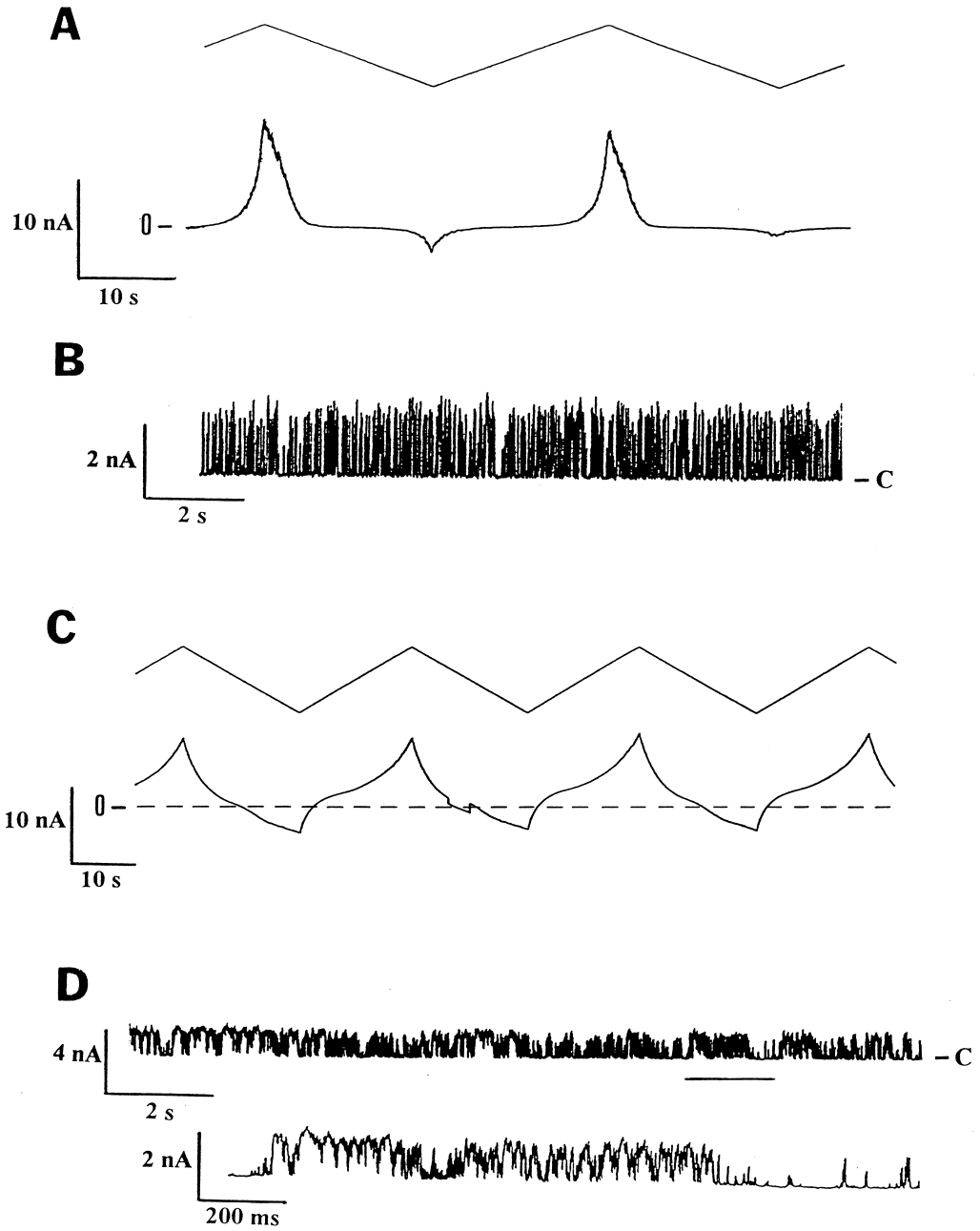

Fig. 3. Macroscopic current responses to 100 mV ramps induced by the dimer **4** at a concentration of 10^{-8} M (A) and by the tetramer **6** at 2×10^{-9} M (C). Single-channel traces are shown in B and D (for derivatives **4** and **6**, respectively) with a zoom for the latter on an approximately 10 times slower time base. Steady-state applied voltage = 50 mV. Openings are upward deflections.

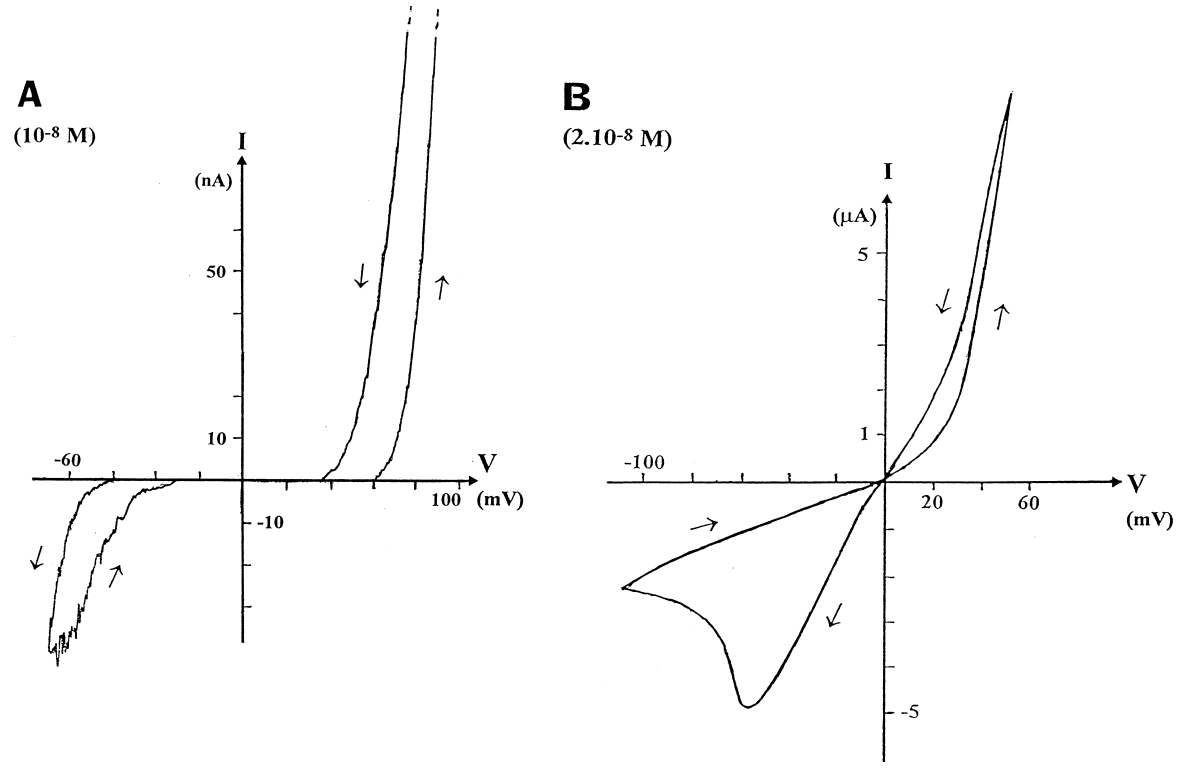

Fig. 4. Macroscopic current–voltage (*I–V*) curves induced by dimer **5** (with an intervening Ala between the two branching Lys) in 1 M KCl at peptide aqueous concentrations of 10^{-8} M (A) and 2×10^{-8} M (B). Arrows indicate parts of the responses associated with the ascending and descending limbs of the voltage ramps. Note the greatly increased current range and the drastic change of pattern in curve B, with the development of a 'negative resistance' branch.

alamethicin was seen, i.e. a steep exponential branch developing towards the extremity of the positive limb of the voltage ramps. Nevertheless there are interesting and significant quantitative differences. First, the addition of the C-terminal three hydrophobic residues in derivative **2**, greatly enhanced membrane affinity since the current density in B is nearly ten times that in A, despite a reduced peptide concentration. Second, whereas the voltage-dependence as estimated by V_e, the voltage increment producing an *e*-fold change in conductance of the exponential branch, was only 10 mV for **1**, it was back to the normal value of 6 mV, typical for native alamethicin [27], with derivative **2**. A full analysis of the concentration-dependence of macroscopic conductance induced by alamethicin(1–17)-AUA (**2**) indicated characteristic voltages $V_{c1} = 143$ mV, and $V_{c2} = 77$ mV to reach a reference conductance of 120 nS at concentrations 10^{-7} M and 3×10^{-7} M, i.e. a voltage shift of $V_a = 60$ mV for an *e*-fold change in concentration. Applying the relation $\langle N\rangle = V_a/V_e$, derived for alamethicin [8] yielded the apparent number of monomers for conducting aggregate, $\langle N\rangle = 10$.

Monomer **3** yielded a similar macroscopic conductance behaviour as alamethicin(1–17) (**1**) although the presence of the linker seems to increase membrane affinity since equivalent concentrations gave a ten times higher current. A different and quite untypical behaviour is observed both for dimer **4** and tetramer **6** containing contiguous lysines in the template. As shown in Fig. 3A and C, the rising phase of macroscopic currents is greatly slowed down and the falling phase is steeper, such that now hystereses (usually reflecting mean channel duration) between the limbs are reversed. Also, although hardly resolved, only one single-channel conductance level of very high amplitude (ca. 40 nS) is observed.

Usual macroscopic *I–V* curves are retrieved when the lysines in the linker are separated by an alanine (Fig. 1, dimer **5**). As shown in Fig. 4A, a typical and asymmetrical *I–V* curve with a high voltage dependence ($V_e = 7$ mV), can be recorded with dimer **5** at

the concentration 10^{-8} M. Doubling the concentration always in the *cis*-side (Fig. 4B), immediately leads to both a greatly increased current–density (note that the latter is now about 10^3 higher than with derivative **1** in Fig. 2A) and the development of a 'negative resistance' branch in the negative quadrant of *I–V* curves. Indeed, along this branch, the current is reduced with increasingly negative voltage giving a peak that is a standard characteristic of excitable membranes [28]. As shown by Fig. 5, the single-channel pattern is now quite different from that of alamethicin: only one open state was recorded in agreement with the stabilising effect expected from such oligomers although the kinetics were still fast, when compared to other recent alamethicin dimers [15].

4. Discussion

All the macroscopic conductance parameters issued from alamethicin(1–17) (**2**) are strictly identical to those of alamethicin in the same experimental conditions [27]. Thus, the replacement of the last three alamethicin residues EQ-Pheol by AUA-OH is of no consequence as far as macroscopic conductance is concerned, confirming that the C-terminal part (after proline 14) of alamethicin has little specific involvement in channel formation. This extends earlier findings with synthetic analogues of alamethicin where all U residues were replaced by L residues [29] and suggests a relatively wide outer mouth for the conducting bundle, in agreement with molecular modelling studies [30]. It was previously shown that the N-terminal part, up to around Pro-14, is more likely to make up the pore lining since selected substitutions in this part affect conductance parameters [31].

The results with dimer **4** and tetramer **6** argue for significantly distorted conducting aggregates, or in any case, quite different from those of alamethicin. The very large observed conductance may represent some transient, detergent-like disruption of the bilayer. Note, however, that no dielectric breakdown occurs and the reversibility of macroscopic responses. In any case, possibly reflecting enhanced helicity (see e.g. [20]), membrane affinity is greatly enhanced with these oligomers since similar current

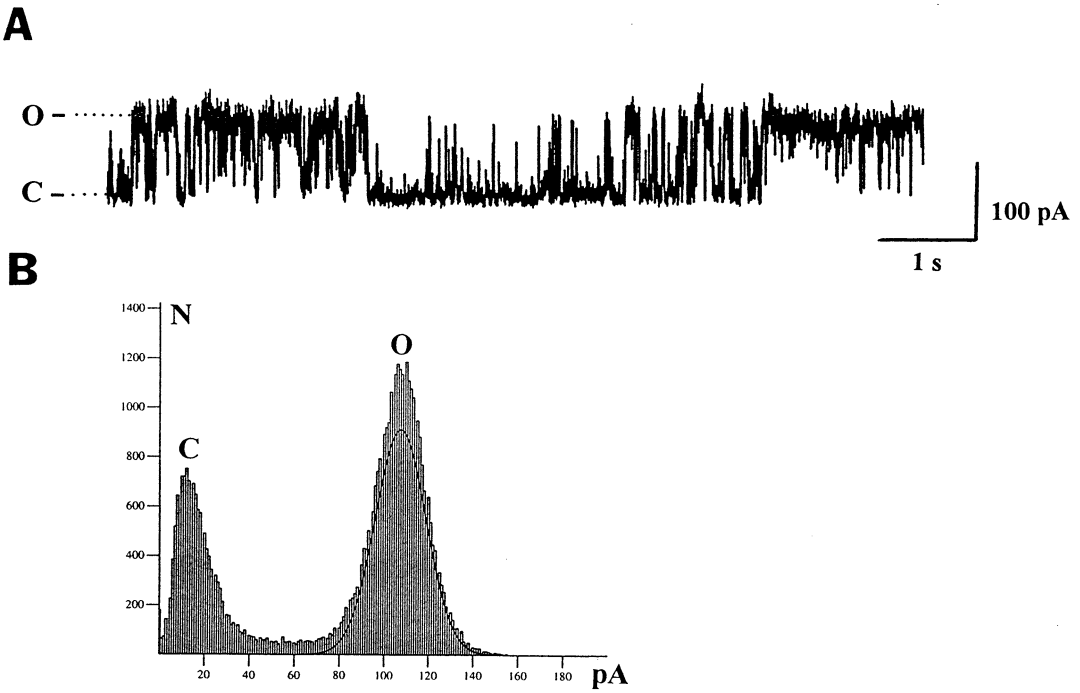

Fig. 5. Single-channel activity induced by dimer **5** at an applied voltage of +25 mV (A). Closed and open state currents are depicted by C and O, respectively. The associated amplitude histogram is shown in B, disclosing a single open state of 95 pA, i.e. a conductance of 3.8 nS (open probability P_o 0.6).

densities are achieved with progressively reduced derivative concentrations from about 10^{-7} M for the monomer **3** to 10^{-8} M and 10^{-9} M for dimer **4** and tetramer **6**, respectively.

The insertion of an alanine between the two lysines presumably allows enough flexibility to the transmembrane alamethicin motifs to optimally align in the bilayer. Under the influence of the electric field, conducting aggregates (of dimer **5**) behave essentially as alamethicin monomers, at least as far as macroscopic conductances are concerned. Although rapidly fluctuating between closed and open states, the channels seem to adopt a fixed geometry since only one single-channel level can be recorded, thus without the usual interplay between a conducting nucleus and available monomers. The pore would be made up of four such dimers **5** since the conductance they induced (3.8 nS) is similar to that developed by an alamethicin heptamer or octamer (depending whether the first conducting state is assumed to result from a trimer or tetramer, respectively) which are two of the most probable conducting bundle in this type of bilayers from an analysis of both macroscopic and single-channel data [27].

Finally, it is remarkable that the development of the negative resistance peak can be achieved at concentrations much lower (two orders of magnitude) that with alamethicin per se [2] and without the addition of polybasic peptides [1]. Negative resistance is a 'steady-state signature' of excitable systems able to develop regenerative responses or action potentials when stimulated above a threshold in current-clamp conditions [28]. Excitability and bistability phenomena with the alamethicin–protamine system were first described some 30 years ago [1], but the molecular interpretation was partly based on a carrier mechanism that is now ruled out for alamethicin. By analogy with 'active' electronic devices such as tunnel diodes, a phenomenological theory was proposed by the same authors [32] assuming: "(1) a free energy difference (ΔF) between two stable channel configurations of different conductivities...; and (2) this ΔF, which can be changed by the applied voltage, determines the number of channels existing in either state. This process... obey Boltzmann statistics". Current–voltage curves were calculated and the sign of ΔF then simply determined whether the system is in the low (rectifier-like) or high (associated with negative resistance) conductance state.

In summary, the chemical synthesis strategy employed in this work allowed to conveniently assay the influence of various linkers bearing shortened alamethicin motifs on the conductances induced in planar bilayers. The results clearly show the minimal requirements to be met for allowing sufficient flexibility with a concomitant high-voltage dependence that is typical of the parent molecule and the drastic reduction in efficient concentrations, especially in developing the interesting feature of negative resistance.

Acknowledgements

M.T.L. acknowledges financial support from the Polish–American M. Sklodowska-Curie Fund II (Grant MZ/HHS-94-168). H.D. expresses many thanks to Mark Sansom (Laboratory of Molecular Biophysics, Oxford University) for sharing with him some of the samples used in this study and for access to his conductance set-up.

References

[1] P. Mueller, D.O. Rudin, Nature 217 (1968) 713–719.
[2] M. Eisenberg, J.E. Hall, C.A. Mead, J. Membr. Biol. 14 (1973) 143–176.
[3] G. Boheim, J. Membr. Biol. 19 (1974) 277–303.
[4] G.A. Woolley, B.A. Wallace, J. Membr. Biol. 129 (1992) 109–136.
[5] M.S.P. Sansom, Eur. Biophys. J. 22 (1993) 105–124.
[6] D.S. Cafiso, Annu. Rev. Biophys. Biomol. Struct. 23 (1994) 141–165.
[7] L.G.M. Gordon, D.A. Haydon, Phil. Trans. R. Soc. London Ser. B 270 (1975) 433–447.
[8] J.E. Hall, I. Vodyanoy, T.M. Balasubramanian, G.R. Marshall, Biophys. J. 45 (1984) 233–247.
[9] H.A. Kolb, G. Boheim, J. Membr. Biol. 38 (1978) 151–191.
[10] W. Hanke, G. Boheim, Biochim. Biophys. Acta 596 (1980) 456–462.
[11] G. Baumann, P. Mueller, J. Supramol. Struct. 2 (1974) 538–557.
[12] M.S.P. Sansom, Prog. Biophys. Mol. Biol. 55 (1991) 139–235.
[13] G.R. Marshall, D.D. Beusen, in: M. Blank, I. Vodyanoy (Eds.), Biomembrane Electrochemistry, Advances in Chemistry Series, Vol. 235, American Chemical Society, 1994, pp. 259–314.

[14] I. Vodyanoy, G.R. Marshall, F. Chiu, Biophys. J. 55 (1989) 333A.
[15] S. You, S. Peng, L. Lien, J. Breed, M.S.P. Sansom, G.A. Woolley, Biochemistry 35 (1996) 6225–6232.
[16] A. Matsubara, K. Asami, A. Akagi, N. Nishino, Chem. Commun. (1996) 2069-2070.
[17] G. Tuchscherer, M. Mutter, J. Biotechnol. 41 (1995) 197–210.
[18] A. Grove, J.M. Tomich, T. Iwamoto, M. Montal, Drugs Dev. 2 (1993) 21–34.
[19] M. Oblatt Montal, T. Iwamoto, J.M. Tomich, M. Montal, FEBS Lett. 320 (1993) 261–266.
[20] A.K. Wong, M.P. Jacobsen, D.J. Winzor, D.P. Fairlie, J. Am. Chem. Soc. 120 (1998) 3836–3841.
[21] U. Slomczynska, J. Zabrocki, K. Kaczmarek, M.T. Leplawy, D.D. Beusen, G.R. Marshall, Biopolymers 32 (1992) 1461–1470.
[22] T.M. Balasubramanian, N.C.E. Kendrick, M. Taylor, G.R. Marshall, J.E. Hall, I. Vodyanoy, F. Reusser, J. Am. Chem. Soc. 103 (1981) 6127–6132.
[23] R. Nagaraj, P. Balaram, Tetrahedron 37 (1981) 1263–1270.
[24] H. Schmitt, G. Jung, Liebigs Ann. Chem. (1985) 321-344.
[25] K. Akaji, Y. Tamai, Y. Kiso, Tetrahedron Lett. 36 (1995) 9341–9344.
[26] M. Montal, P. Mueller, Proc. Natl. Acad. Sci. USA 69 (1972) 3561–3566.
[27] C. Kaduk, H. Duclohier, M. Dathe, H. Wenschuh, M. Beyermann, G. Molle, M. Bienert, Biophys. J. 72 (1997) 2151–2159.
[28] G. Grundfest, in: Adelman, W.J. Jr. (Ed.), Biophysics and Physiology of Excitable Membranes, Van Nostrand Rheinhold, 1971, New York, pp. 477–504.
[29] G. Molle, H. Duclohier, S. Julien, G. Spach, Biochim. Biophys. Acta 1064 (1991) 365–369.
[30] J. Breed, I.D. Kerr, G. Molle, H. Duclohier, M.S.P. Sansom, Biochim. Biophys. Acta 1330 (1997) 103–109.
[31] G. Molle, J.-Y. Dugast, G. Spach, H. Duclohier, Biophys. J. 70 (1996) 1669–1675.
[32] P. Mueller, D.O. Rudin, J. Theor. Biol. 4 (1963) 268–280.